Postprint of: Agricultural and Forest Meteorology 218-219: 92-101 (2016)

The dynamics of radial sap flux density reflects changes in stomatal conductance in response to soil and air water deficit

Hernandez-Santana, V.[1], Fernández, J.E.[1], Rodriguez-Dominguez, C.M.[1,2], Romero, R.[1], Diaz-Espejo, A.[1,*]

[1] Irrigation and Crop Ecophysiology Group, Instituto de Recursos Naturales y Agrobiología de Sevilla (IRNAS, CSIC). Avenida Reina Mercedes, nº 10, 41012-Sevilla, Spain

[2] Departamento de Biología Vegetal y Ecología, Universidad de Sevilla, Sevilla, Spain

* Corresponding author. a.diaz@csic.es. +34 954624711

ABSTRACT

Water scarcity in semiarid regions of Europe threatens the sustainability of fruit tree orchards unless irrigation water is optimized and scheduled in deficit irrigation strategies. Stomatal conductance (g_s) is one of the best indicators of plant water stress, since it is placed in the crossroad between water and CO_2 fluxes at the leaf level. Unfortunately, it is not possible to measure g_s automatically and continuously, which reduces its potential for irrigation scheduling. In this work we examined the use of sap flux density (J_s) in the outer rings of the sapwood of olive trees as a surrogate of g_s. The working hypothesis was that as olive trees are well-coupled to atmosphere because of their small leaves, the ratio of J_s to air vapor pressure deficit (D) should correlate well with the dynamics of g_s in the canopy. It was also expected that current year, sun exposed leaves were mainly connected to the outer rings of the sapwood, and the oldest, shaded leaves to the inner rings. This was tested by measuring g_s in new, sun-exposed leaves *vs* g_s in old, shaded leaves. Both hypotheses were contrasted and our results confirmed that g_s can be estimated from J_s/D (R^2 of the relationships were always higher than 0.8). A wide range of estimated g_s values (0.350-0.025 mol m^{-2} s^{-1}) were derived from J_s measurements in an olive orchard under three different irrigation regimes. Results were satisfactory and open the possibility of applying this method to estimate g_s and use it either as a reliable water stress indicator or in transpiration and photosynthesis models applied to fruit tree orchards under a wide range of water stress conditions.

Keywords: olive; stomatal conductance; water stress; sap flow; irrigation scheduling

INTRODUCTION

Expected climate conditions in the Mediterranean area demand an increasing use of sustainable water use practices in agriculture, such as deficit irrigation (DI). The correct use of the most successful deficit irrigation strategies, such as regulated deficit irrigation (RDI; Chalmers et al., 1981) requires both a good understanding of physiological mechanisms involved in the response of plants to water stress, and the use of reliable and sensitive indicators of water stress (Fernández, 2014a). For the latter, special attention has been paid to plant-based methods, since plant measurements have the advantage of integrating the soil and atmospheric water status, as well as the response of the plant to the surrounding conditions (Jones, 2004). New methods have been developed for non-destructive, automatic and continuous measurements, such as dendrometers, sap flow and turgor-related probes. These new methods have several advantages compared to conventional plant-based methods, e.g. water potential or stomatal conductance, which are commonly destructive and time and labor consuming (Fernández, 2014b).

Stomatal conductance (g_s) is a good plant-based indicator for irrigation purposes. Besides g_s quick response to increasing water stress, stomatal closure limits photosynthesis (Flexas et al., 2013) and thus, it has important implications for plant function, growth and yield (Brodribb 2009). Indeed, stomatal control is regulated to optimize the outward diffusion of water vapor and the diffusion of CO_2 into the leaf during photosynthesis (Hetherington and Woodward, 2003). However, its use for irrigation scheduling purposes faces a major limitation from the difficulty of being automatically and continuously monitored. Yet g_s can be derived easily from transpiration measurements based on a simplification of the Penman-Monteith equation under certain circumstances, as transpiration proceeds largely at the imposed rate which

depends mainly on atmospheric conditions (McNaughton and Jarvis, 1983). Transpiration values can be estimated from sap flow related measurements. Sap flow methods work automatically and continuously, and are relatively inexpensive and user-friendly compared to other approaches (Wullschleger et al., 1998). Total sap flow or tree transpiration (L h^{-1}) is calculated from upscaling the sap flux density (J_s, mm h^{-1}) measured at discrete single points in the sapwood to tree scale (sapwood or leaf area based). However, J_s is very variable both at different azimuthal locations (López-Bernal et al., 2010) and along the radial profile (Swanson, 1994). It has also been observed to change not only in the short-term (Ford et al., 2004b; Poyatos et al., 2007; Hernandez-Santana et al., 2008), but also in the long-term as new xylem forms (Beauchamp et al., 2012). The azimuthal variability is a source of uncertainties in the upscaling to the whole tree transpiration, as several authors have reported (López-Bernal et al., 2010; Vandegehuchte et al., 2012). However, the radial variability provides information about the water status of the plant, useful for irrigation scheduling. Indeed, a number of factors have been reported as responsible for the dynamic radial variation of J_s, including changes in soil water status (Fernández et al., 2001; Nadezhdina et al., 2007 but see Beauchamp et al., 2012), mobilization of water stored in the inner sapwood (Ford et al., 2004a,b) to compensate for cavitation in the outer rings (Granier et al., 1994; Ford et al., 2004b; Poyatos et al., 2007), water uptake from deep roots (Nadezhdina et al., 2007; Cermak et al., 2008), stomatal closure in the exposed leaves in response to evaporative demand (Fernández et al., 2001; Ford et al., 2004b, Nadezhdina et al., 2002; Poyatos et al., 2007; Hernandez-Santana et al., 2008), distribution of foliage in the crown (Fiora and Cescatti, 2008) and changes in the distribution of incident radiation across the canopy (Ford et al., 2004a; Jimenez et al., 2000).

Specifically, quick variations in J_s radial profiles have been proposed to be explained by a differential transpiration between the older leaves, lower in the canopy and thus increasingly

shaded, and the younger, better illuminated leaves, in the upper parts of the canopy. The older leaves would be hydraulically connected to older, inner sapwood and the younger to outer sapwood (Dye et al., 1991; Jiménez et al., 2000; Fiora and Cescatti, 2008). Despite all the evidences and hypotheses proposed, however, there has been no direct assessment, to the best of our knowledge, of the link between g_s in sun and shade leaves with differential J_s in younger and older sapwood areas of the same conductive organ, respectively. It is clear that the xylem of leaves produced during a given year is connected preferentially to the stem xylem formed on the same year but little is known on how ageing leaves maintain a connection with the xylem and phloem as the stem grows (Maton and Gartner, 2005). In this study we aimed to assess the links between J_s measured in the trunk of olive trees, at different depths below the cambium, and concomitant g_s measurements in leaves of different age and locations in the canopy. Our objectives were: (i) to determine if there is a robust relationship between g_s measured in the tree canopy and J_s measured in tree trunk, (ii) to assess whether changes in the radial profile of J_s can be attributed to changes in the behavior of g_s of sun-exposed, new leaves (hereafter reported as SUN leaves) *vs*. g_s of shade, old leaves (hereafter SHADE leaves) in response to water stress, and (iii) to determine whether changes in the radial profile of J_s mediated by g_s can be related to changes in soil water deficit and air vapor pressure deficit (*D*). Our findings could have a great potential in agriculture, because of the usefulness of g_s as water stress indicator to schedule irrigation (Jones, 2004).

MATERIALS AND METHODS

Experimental conditions

Measurements were made at two experimental orchards in different years. A summary of the measurements of each orchard is presented in Table 1. Both orchards are located in an area

with Mediterranean climate. Annual average precipitation and potential evapotranspiration are 534.0 mm and 1541.5 mm, respectively, with hardly any rainfall during the summer months. Average maximum and minimum air temperatures in the area are 24.9 °C and 10.7 °C, respectively (period 2002-2012). The hottest months are July and August. Average maximum temperatures over 40 °C are recorded nearly every year, with peak values rarely over 45 °C.

The first set of measurements were conducted in 1998 in the olive orchard of La Hampa, the experimental farm of the Instituto de Recursos Naturales y Agrobiología (IRNAS, CSIC), close to Coria del Río, Seville (latitude 37º17' N, longitude 6º3' W, altitude 30 m). The trees were 30-year-old 'Manzanilla de Sevilla' olive trees (*Olea europaea* L.) at 7 m x 5 m spacing (286 trees ha^{-1}). The soil of the orchard is a sandy loam (Xerochrept) of variable depth. Two irrigation treatments were studied: well-watered trees (WW), in which trees were irrigated daily to replace the crop water needs, and rain-fed trees (WS) (see details in Fernández et al., 2003). Irrigation needs (IN) in the WW trees were calculated as $IN=ET_c-P_e$, being ET_c the maximum potential crop evapotranspiration calculated with the crop coefficient approach (Allen et al., 1998) and P_e the effective precipitation calculated as 75% of the precipitation recorded in the orchard (Orgaz and Fereres, 2001).

The second set of measurements were made in a commercial hedgerow olive orchard, Sanabria, in southwest Spain (37° 15´ N, -5° 48´ W). Trees (*Olea europaea* L., cv Arbequina) were planted in 2007, at 4 m × 1.5 m (1667 trees ha^{-1}), in rows oriented N–NE to S–SW. Measurements were made in the 2012 summer, when trees were 2.40 m tall and the crown was 1.96 m x 1.5 m on average. The studied trees were central individuals located in 12 m × 16 m plots with 24 border trees. We had three irrigation treatments, FI, 60RDI and 30RDI, with four plots per treatment, arranged in a randomized block design. In the FI plots daily irrigation was supplied to replace 100% of IN calculated, once again, with the crop coefficient approach. In the 60RDI and 30RDI plots we applied two regulated deficit irrigation treatments in which

134 total irrigation supplies amounted to 60% and 30% of IN, respectively. In May and June RDI
135 trees were irrigated daily. In July and August, however, trees were irrigated only two days per
136 week in 60RDI and one day per week in 30RDI. Details are given in Fernández et al. (2011).

137

138 *Sap flux density measurements*

139 The Compensation Heat Pulse (CHP) method (Green et al., 2003) was used to derive sap flux
140 density (J_s, mm h^{-1}) values within the sapwood of the sampled trees (Tranzflo NZ Ltd.,
141 Palmerston North, New Zealand) in both sets of experiments. Briefly, CHP consists on
142 measuring the time for the temperature difference registered by two temperatures probes
143 situated 10 mm downstream and 5 mm upstream of a heater probe to become 0 after
144 releasing a heat pulse. Details on the calibration and testing of the technique for the olive tree,
145 as well as on data analysis, are given in Fernández et al. (2001, 2006). At La Hampa
146 experimental farm three sets of heat-pulse probes were installed at three equal spacings
147 around the azimuth of control and water stressed tree trunks at 0.5 - 0.6 m aboveground. Two
148 trees were instrumented for each water treatment. Each probe had four thermocouples, at 5,
149 12, 22 and 35 mm below the cambium. Heat pulses (60 J; 60 W over 1 s) were applied once
150 every 30 min. The data were collected in 1998, from March 24 to the end of September, with a
151 Campbell CR10X data logger (Campell Scientific Inc., USA). At the Sanabria experimental
152 orchard one central tree per plot, in three plots per treatment, was instrumented with two sap
153 flow probe sets, at the east and west facing sides of the trunk and at 0.3 - 0.4 m aboveground.
154 Each temperature probe measured the sap velocity at 5, 10, 15 and 20 mm below the
155 cambium. Measurements were made every half hour, for the entire experimental period (from
156 May 4 to October 21, 2012). A CR10X datalogger connected to a AM25T multiplexer (Campbell,
157 Campbell Scientific Ltd., Shepshed, UK) were used to release the heat pulses and collect the
158 probe outputs. Sap flux density measured in the trunk at 5 mm depth from the cambium will

159 be reported as J_{S1} whereas J_s determined at 10 mm in Sanabria orchard and 12 mm in La
160 Hampa farm will be reported hereafter as J_{S2}.

161 *Meteorological conditions and soil water content*

162 Main weather variables in both orchards were monitored by a weather station (Campbell
163 Scientific Ltd., Shepshed, UK) located in the center of each experimental area. Meteorological
164 sensors were between 2 m and 3 m above the canopies. The station recorded 30 min average
165 values of wind speed (u), air temperature (T_a), air humidity (RH_a), global solar radiation (R_s), net
166 radiation (R_n), photosynthetically active radiation (PAR), and precipitation (P). At La Hampa
167 orchard the volumetric soil water content (ϑ_v) was estimated with a neutron probe (Troxler
168 3300, Research Triangle Park, North Carolina, USA) measuring every 0.1 m, from 0.3 m down
169 to the maximum depth explored by the roots (see Fernandez et al., 2003 for details). In the top
170 soil layers the volumetric soil water content (ϑ_v) was measured by gravimetry. At the Sanabria
171 orchard ϑ_v was measured with a Profile probe (Delta-T Devices Ltd, Cambridge, UK) and two
172 access tubes per plot, at ca. 0.5 m from the tree trunk. One of the access tubes was at 0.1 m
173 from a dripper, i.e. in the soil volume wetted by irrigation. The other was at 0.4 m from the
174 dripper, i.e. in drying soil during the irrigation season. In each access tube we measured ϑ_v at
175 0.1, 0.2, 0.3, 0.4, 0.6 and 1.0 m depth, 1–2 times per week, all along the irrigation season. The
176 Profile probe was calibrated in situ by Fernández et al. (2011). We used the collected ϑ_v values
177 to calculate the relative extractable water (REW) in the root zone as REW=(R-R_{min})/(R_{max}-
178 R_{min}),where R (mm) is the actual soil water content, R_{min} (mm) the minimum soil water content
179 measured during the experiments, and R_{max} (mm) is the soil water content at field capacity.

180 *Stomatal conductance*

181 Measurements of stomatal conductance (g_s) in La Hampa were made in three leaves of each
182 instrumented tree on DOY 131. Two replicates per tree were taken by using a LI-6400 portable

183 photosynthesis system (LI-COR, Lincoln NE, USA) with a 2 cm × 3 cm standard chamber. SUN
184 and SHADE leaves were selected depending on their age, current or last-year grown, which can
185 be clearly determined from their location in the shoot. SUN and SHADE leaves had an average
186 PPFD at midday of 934 ± 95.2 μmol m^{-2} s^{-1} and 267 ± 43.8 μmol m^{-2} s^{-1} Measurements were
187 made at 8.30 GMT when g_s was at its maximum (Fernández et al., 1997). At the Sanabria
188 orchard g_s measurements were conducted in trees of the three irrigation treatments, next to
189 the ones where J_s was measured (one tree per plot, in three plots out of the four plots per
190 treatment). Measurements were conducted as described for La Hampa, every two weeks
191 during the whole irrigation season. In all cases measurements were taken at ambient light and
192 CO_2 conditions. Additional measurements of g_s were conducted in one FI plot and in one 30RDI
193 plot, on two days when the 30RDI trees were under different soil water conditions (day of year
194 – DOY – 177, ϑ_v = 0.233 cm^3 cm^{-3}; DOY 216, ϑ_v = 0.174 cm^3 cm^{-3}). In those plots g_s was
195 determined every 1.5 h from dawn to dusk, in four SUN and four SHADE leaves from the outer
196 and inner part of the canopy, respectively, facing SE, at ca. 1.5 m above ground, in one 30RDI
197 and one FI tree, both instrumented with sap flow sensors. Hereafter these trees will be
198 referred to as the water stressed tree (WS) and the well-watered tree (WW), respectively. SUN
199 and SHADE leaves had an average PPFD at midday of 588 ± 81.1 μmol m^{-2} s^{-1} and 148 ± 19.9
200 μmol m^{-2} s^{-1} in DOY 177 and 742 ± 219.3 μmol m^{-2} s^{-1} and 114 ± 44.9 μmol m^{-2} s^{-1} in DOY 216.

201 A Student´s t test was used to assess differences between mean values of g_s by canopy
202 exposure (SUN and SHADE g_s) after passing the normality test (Shapiro-Wilk). Significant
203 differences were reported at α = 0.05. *D* was Ln-transformed so we obtained linear
204 relationships, easier to interpret. Statistical analyses were conducted with SigmaPlot (version
205 12.0, Systat Software, Inc., San Jose, California, USA).

206

207 **RESULTS**

208 *Relationship between radial profiles of sap flux density and stomatal conductance*

209 Figure 1 depicts the dynamic shape of the radial profile of J_s in an olive tree trunk. Data shown
210 in the figure were collected on June 27 of 2012, a day when g_s was measured along the day
211 and both WW and WS trees were not water-stressed. As *D* increased early morning (from 8.00
212 to 11.00 GMT, Fig. 1a), J_s values increased at all explored xylem depths (Fig. 1b). However,
213 between 11:00 GMT and 15:00 GMT, when *D* was still increasing, J_{S2} increased but J_{S1}
214 decreased. Furthermore, the J_{S2} increase observed from 11.00 to 15.00 GMT was not
215 correlated to the magnitude of *D* increase, which was even larger to the one observed from
216 8:00 GMT to 11:00 GMT. These results could be explained by J_s being limited by decreasing g_s
217 from early in the morning, which counterbalances the driving force of the increasing
218 atmospheric demand. This supports our hypothesis on the role of stomatal regulation in
219 transpiration and its effect on J_s profiles in the trunk, as reported in previous works mentioned
220 in the Introduction. The rest of this section is devoted to test this hypothesis.

221 To test the relationship between g_s and J_s we conducted regressions between mean g_s values
222 of SUN and SHADE leaves and J_{s1} and J_{s2} divided by *D* to remove the *D* effect. All relationships
223 established between g_s and J_s/D were highly significant (Fig. 2) regardless of the water deficit
224 or the leaf exposure. These relationships were found in two unrelated experiments with trees
225 of different age and cultivar (5-year-old 'Arbequina' trees in Sanabria and 30-year-old
226 'Manzanilla' trees at La Hampa). The relationships were unique even on days with different
227 water deficits (Fig. 2a,b). In all cases the coefficients of determination were higher than 0.80
228 and highly significant ($P<0.0001$). Relationships were found to be different for SUN and SHADE
229 leaves, suggesting a different behavior in both populations of leaves in response to
230 environmental conditions. Moreover, these relationships showed around a 10% better fit on
231 average when J_{S1} was related to SUN leaves, and J_{S2} with SHADE leaves (Fig. 2), than J_{S1} with
232 SHADE leaves and J_{S2} with SUN leaves (data not shown).

233 The response of g_s measured in SUN and SHADE leaves to Ln*D* (Fig. 3) help us to understand
234 the role of main environmental drivers in the g_s - J_s relationship, and to further assess the
235 effect of Ln*D* on the J_{S1}/J_{S2} ratio observed at different levels of soil water deficit in both WW
236 and WS trees (Fig. 4). Both types of leaves responded to increasing *D* by reducing their g_s (Fig.
237 3). The response was greater in SUN leaves than in SHADE leaves, especially in WW trees (Fig.
238 3a,c). In the WS trees similar values of g_s were found in SUN and SHADE leaves (Fig. 3b,d),
239 suggesting that soil water deficit induced a larger depression in g_s of SUN leaves, which are
240 more related to the younger, more exposed leaves. There was also a hysteresis effect between
241 the high g_s values recorded in the morning and the lower g_s measured in the afternoon in the
242 SUN leaves of the WW tree at Sanabria (Fig. 3a). All g_s measurements were conducted on the
243 east part of the canopies, such that the hysteresis could have been caused by changes on
244 radiation interception along the day. Accordingly to the derived Ln*D*-g_s relationships, the g_s
245 sensitivity decrease to *D* (magnitude of the reduction in g_s with increasing *D*; Oren et al., 1999)
246 was more pronounced in SUN leaves than in SHADE leaves (67% in Sanabria orchard and 86%
247 in La Hampa farm) in the WW tree than in the WS tree (27% in Sanabria orchard and 44% in La
248 Hampa farm). We used the g_s values of central day hours from 8.30 to 15.30 GMT with the
249 data of Sanabria orchard and from 8.00 to 17.00 GMT in La Hampa farm to avoid hysteresis
250 effect.

251 Significant relationships were found between J_{S1}/J_{S2} ratios and Ln*D* (Fig. 4), independently of
252 tree age and cultivar. This consistency and robustness was likely a consequence of both the
253 different sensitivity of g_s to *D* of SUN and SHADE leaves (as seen in Fig. 3) and the correlation
254 found between g_s and J_{S1} and SUN leaves and J_{S2} and SHADE leaves (Fig. 2). For the Sanabria
255 orchard, where two different days were analyzed simultaneously, the slopes of J_{S1}/J_{S2} *vs* Ln*D*
256 were very similar between the two studied days both in the WW (Fig. 4a) and WS tree (Fig.
257 4b). The decrease of J_{S1}/J_{S2} with higher *D* values in both trees could be explained by the
258 different response of g_s to *D* in SUN and SHADE leaves (Fig. 3). However, while for the WW tree

the two curves were indistinguishable, in the WS tree the J_{S1}/J_{S2} ratios were higher for the D range occurring on the day with no soil water deficit (DOY 177) than on the day with soil water deficit (DOY 216). This could have been a consequence of a proportionally greater decrease in J_{S1} than in J_{S2} under water stress conditions.

Testing the seasonal changes of J_s/D and its representativeness of g_s

After demonstrating the correlation between the dynamics of J_s in the outer xylem of the trunk and that of g_s in the canopy, we intended to infer the seasonal changes of g_s in the Sanabria orchard, where we had established three water treatments. The D and R_s courses for a growing season (May to September) are shown in Fig. 5a,b. The figure also shows REW values for the three treatments (Fig. 5c). We calculated the time course of g_s through the 170 days represented in the figure (from DOY 125 to DOY 295), for the three irrigation treatments, using the inverse relationship of g_s-J_s/D, (Fig. 6). We used SUN and J_{S1} and not SHADE and J_{S2} because g_s measurements at 8:30 GMT were only conducted in SUN leaves. The J_s/D- g_s relationships (Fig. 2) indicated a constant relationship for each tree regardless the level of water stress. Thus, we estimated the ratio between g_s and J_s/D for each tree using data from the first measurement day only (in May, calibration dataset). Then we used that single ratio value to calculate g_s for the rest of the season (validation dataset).

Usually J_s/D values derived from the outputs of sap flow probes installed in the east side of the trunk fitted better with g_s than values from the west-oriented probes (data not shown). Likely, this was because g_s was always measured in the east side of the canopy. The seasonal course of the calculated g_s was mainly driven by D and REW (Fig. 6a, b, c). Values of g_s decreased as D increased. On the contrary, g_s decreased with REW. Indeed, the dynamics of g_s were dependent on the irrigation treatment. In the studied period, FI trees were irrigated daily, while 60RDI and 30RDI trees were often irrigated just once or twice per week. Soil water availability explains that g_s showed lower values in these two deficit irrigated trees than in the

FI trees. It was also observed that calculated g_s in the 60RDI tree was higher for the period with daily irrigation (DOY 165-185) than when water was supplied just once per week (DOY 185-210). For all treatments, calculated g_s values using J_{S1} agreed reasonably well with measured g_s values (Fig. 7), for a wide g_s range (0.350 mol m^{-2} s^{-1} to 0.025 mol m^{-2} s^{-1}) , as shown by the R^2 values (0.93, 0.83 and 0.81 for trees of FI, 60RDI and 30RDI trees, respectively).

DISCUSSION

Do radial profiles of sap flow in the tree trunk reflect stomata dynamics in the canopy?

Our results confirm our hypothesis that the diurnal dynamics of J_s in the olive trunk reflect directly g_s dynamics at leaves in the canopy. The robust relationships found between g_s and J_s/D using measurements under different soil and atmospheric water conditions highlights the fact that unique relationships between these variables can be established regardless the environmental conditions (Fig. 2). These relationships were obtained with two olive cultivars of different age growing in different orchards, extending the confidence on our results further. In addition to test for any potential influence of the cultivar in the results obtained, both orchards represent two different systems in which the structure of the canopy (hedgerow at Sanabria *vs* isolated trees at La Hampa) and age and size of the trees (larger at La Hampa with more irregular trunk sections than at Sanabria) were clearly contrasted. This minimizes the concerns about issues related to the assumption of a complete coupling to the atmosphere and with the maintenance of the relationship between J_s in irregular trunks and g_s in the canopy. Although the relationships plotted in Fig. 2 are empirical, they are physiologically based and rest on the well documented fact that in olive trees most of the transpiration is driven by *D* (Moreno et al, 1995; Tognetti et al., 2009). Under these conditions of high coupling to the atmosphere, stomata can exert a fine control of transpiration, being changes on stomatal closure directly reflected in the transpiration flux estimated from sap flow related measurements in the tree trunk. This would explain the robust J_s/D-g_s relationships shown in

309 Fig. 2 for a wide range of g_s and conditions. It is significant that the increase in *D* between
310 11:00 GMT and 15:00 GMT only represented a small increment in J_{S2}, but a decrease in J_{S1}. This
311 can be explained if g_s decreased in SUN leaves enough to compensate for the increase in *D*.
312 This is also supported by the response of g_s to *D* depicted in Fig. 3, in which it is shown that
313 SUN and SHADED leaves respond differently to increasing atmospheric demands. Moreover,
314 the agreement between J_s and g_s was, on average, ca. 10% better when J_s values derived from
315 measurements at 5 mm below the cambium, i.e. in the outer part of xylem where new tissues
316 are, were related to g_s measured in SUN leaves than when related to g_s measurements in
317 SHADE leaves. These results support the hypothesis that SUN leaves are hydraulically
318 connected mostly to the newer, outer sapwood, while the SHADE leaves are connected to
319 older, inner sapwood. According to Granier et al. (1994), this differential connection implies no
320 significant radial water transport in the olive xylem. In agreement with that, Jiménez et al.
321 (2000) reported that high sap flow values in outer sapwood layers are to some extent linked to
322 high transpiration rates of the well-illuminated upper canopy, whereas lower sap flow rates in
323 the inner sapwood layers reflected the low transpiration rates of the partially shaded, lower
324 parts of the canopy. Indeed, studies on leaf gas exchange in Mediterranean species showed
325 that g_s was much lower in needles of *Abies pinsapo* (Sancho-Knapik et al., 2014) or leaves of
326 *Eucryphia cordifolia* (Morales et al., 2014) in the shade than in the sun. The association of sap
327 fluxes in the outer rings with new leaves and inner ones with older leaves would mean a
328 compartmentalization of the hydraulic system that suggest a low interconnectivity among
329 xylem vessels. Plants adapted to dry environments are known to have a low hydraulic
330 conductivity, as it is the case of olive (Diaz-Espejo et al., 2012; Tognetti et al., 2009). Clearly,
331 additional information seems to be necessary before establishing the fundamentals of leaf-
332 stem xylem connections, which, as suggested in this study, might be of capital importance to
333 understand the functioning of whole trees.

334

335 If stomata of SUN leaves respond more markedly to *D* than stomata of SHADE leaves (Fig. 3),
336 and provided that there is a preferential hydraulic connection between young leaves and the
337 most external vessels in the xylem, as Fig. 2 suggests, reduction in the J_{S1}/J_{S2} ratio as *D*
338 increased can be expected. This was the case, as shown in Fig. 4. The slope and y-intercept of
339 the relationship between J_{S1}/J_{S2} and *D* hardly varied among days in WW trees (Fig. 4a,c).
340 However, under dryer situations the y-intercept varied in WS trees, since more sap appears to
341 be conducted deeper into the sapwood, resulting in a proportionally higher contribution of J_s
342 from deeper sapwood than from outer, newer sapwood. Our results suggest that changes in
343 the recorded J_s radial profiles were likely related to a differential response of g_s between SUN
344 leaves and SHADE leaves to both soil water deficit and *D* (Fig. 2). This is in agreement with
345 diurnal changes in the sap flow profiles reported by Fernandez et al. (2001), also in olive. This
346 species has a low hydraulic conductivity (Diaz-Espejo et al., 2012), and keeps their stomata
347 fully open only in the morning hours when *D* is still low. Later on the day, the stomata close in
348 response to increasing *D*, especially in SUN leaves. This can explain the observed changes in
349 the shape of the recorded diurnal profiles. The greater sensitivity of g_s to *D* of SUN leaves as
350 compared to SHADE leaves was dramatically reduced with water stress (Fig. 2), such that,
351 under dry conditions, the response of g_s to *D* was very similar in SUN and SHADE leaves. Loss of
352 stomatal control in older and more shaded leaves might be explained by two main reasons: (i)
353 a delayed response of stomatal closure to dehydration as leaf ages (as suggested by Fernández
354 et al., 1997) and (ii) a major decoupling from surrounding atmosphere. SHADE leaves are not
355 so well coupled to the atmosphere as SUN leaves, probably because the boundary layer
356 around the leaves is not as easily removed as it is in the outer part of the crown. Thus, SHADE
357 leaves may not respond so well to the surrounding atmospheric conditions. The spatial
358 distribution of leaf-to-air coupling (McNaughton and Jarvis, 1983; Jarvis and McNaughton,
359 1986) within individual plant foliage can determine whether transpiration in sun-exposed and

360 more shaded leaves is differently controlled either by D and g_s (imposed evaporation, strong
361 coupling) or by net radiation (equilibrium evaporation, weak coupling).

362 It has also been reported, for different species and conditions, that, under increasing soil water
363 deficit, flow in the inner xylem remained relatively constant, whereas flow in the outer xylem
364 decreased, resulting in a greater contribution of the inner xylem to total sap flow (Granier et
365 al., 1994; Fernández et al., 2001; Ford et al., 2004b; Nadezhdina et al., 2007). Poyatos et al.
366 (2007) found in pubescent oak a proportionally greater contribution to total trunk flow from
367 the outer xylem during conditions of high evaporative demand, whereas Ford et al. (2004a), in
368 agreement with our results (Figs. 1, 4), found that high evaporative conditions were
369 responsible for the mobilization of water in the inner sapwood of pine trees. An interesting
370 aspect of our results is that the g_s sensitivity to D (the slope of LnD-g_s relationship, according to
371 Oren et al., 1999) decreased in SUN leaves under water deficit conditions to levels of SHADE
372 leaves. Finally, it should be noted that the observed hysteresis due to the time of the day in
373 the LnD-g_s relationship of SUN leaves under well-watered conditions was likely due to the
374 different regime of light interception by the canopy, and reinforces the idea of a close
375 connection between foliage elements and the conductive tissue in the trunk. Hysteresis has
376 also been reported by Poyatos et al. (2007) and Alvarado-Barrientos et al. (2013), among
377 others, and do not affect our conclusions.
378 The major limitation of our approach is the empirical nature of the calibration factor relating
379 J_s/D with g_s. As this relationship is empirical, it could change with tree size or other
380 characteristics of the tree or the canopy. However, we have shown how the calibration factors
381 are similar between different trees, given a similar wood anatomy as it happens within a single
382 species. In our study, we demonstrated that even in orchards where trees are isolated (La
383 Hampa) or planted in hedgerows (Sanabria) the approach works fine. Still, the natural
384 variability between trees and within a single tree is another important point to be considered,
385 as in any ecophysiological study. Other shortcomings of this approach are the mechanisms that

386 can produce time lags between J_s in the trunk and g_s in the canopy such as water storage and
387 fluctuating light conditions (i.e. cloudiness).
388
389 *Use of* J_s/D *to simulate seasonal changes of* g_s *automatically in the field from sap flow data*

390 Our results show that, at least in olive, g_s can be determined from J_s data directly. This way of
391 estimating g_s avoids the J_s up-scaling process in the calculation of tree transpiration to
392 estimate canopy conductance (g_c) as it is commonly done. Former attempts to estimate
393 stomatal conductance from sap flow measurements were based on inverting Penman-
394 Monteith equation. That approach requires the use of absolute values of total plant
395 transpiration, which in turn requires knowing and integrating both the sap flux velocities in the
396 trunk and the total leaf area. Thus, our method avoids the uncertainties derived from the
397 required upscaling from measurements at single points in the trunk to the whole tree
398 (Shinohara et al., 2013). The J_s up-scaling to tree transpiration has been proved to be difficult
399 given the J_s azimuthal and radial variability and the conductive surface area asymmetry in olive
400 (Fernández et al., 2006; Lopez-Bernal et al., 2010; Vandegehuchte et al., 2012; Hernandez-
401 Santana et al. 2015). However, our approach does not require integrating J_s at different
402 locations in the tree trunk. It can be used with a single-point sensor, since only the most
403 external J_s is used. As shown along this study, this approach is sensitive enough to allow us
404 inferring how stomata respond to the two main driving variables of transpiration under water
405 stress: atmospheric and soil water deficit (Fig. 6). Other methods, like Bowen ratio or eddy-
406 covariance, are expensive, need many assumptions and corrections and require intense
407 training. Our results facilitate two interesting applications. First, g_s can be derived from
408 continuous and automatic measurements of J_s, which suggests the possibility of using short-
409 term changes of g_s (through J_s) as a plant-based indicator for irrigation scheduling. We have
410 shown in three different trees under three irrigation treatments that an initial and single
411 calibration was sufficient to derive g_s for the whole season (Fig. 6). This robustness of the

412 relation g_s- J_s/D is also supported by Fig. 2. Our approach is more related to the use of g_s as an
413 indicator of water stress, rather than to estimate the total tree transpiration. However, the
414 inclusion of this estimated g_s in wide-used models of transpiration like Penman-Monteith
415 (Zhang et al., 1997) would help to solve one of the biggest troubles when applying this
416 equation: the effect of water stress. The response of stomata to driving environmental
417 variables has been tried to be modelled by several approaches (Jarvis, 1976; Leuning, 1990;
418 Diaz-Espejo et al., 2012; Peak and Mott, 2011). But a reliable g_s model incorporating
419 mechanistically the response of stomata to water stress is still elusive (Buckley and Mott,
420 2013; Egea et al., 2011). Our results could help to solve this problem since J_s/D was able to
421 track adequately the daily and hourly dynamics of g_s in FI, 60RDI and 30RDI trees, as it is shown
422 in Fig. 6 and Fig. 7. A second application is related to the influence of g_s on photosynthesis.
423 Stomata closure determines, to a large extent, the use of water by fruit trees under water
424 stress conditions, but also CO_2 assimilation rate. Thus, g_s is the main determinant of
425 photosynthesis limitation under water stress conditions (Flexas et al., 2004). Hence, once the
426 course of g_s along the season is known we might be able to estimate net CO_2 assimilation by
427 leaves and to estimate the limitation to photosynthesis imposed by stomata closure. This can
428 be achieved by either applying process-based models of photosynthesis (Diaz-Espejo et al.,
429 2006) or by simple empirical relationships between photosynthesis rate and g_s (Fernández et
430 al., 2008; Medrano et al., 2002). In an agronomical context, the prediction of net CO_2
431 assimilation rate should be a target indicator to assess the effect of water stress on yield. The
432 method we propose would help to overcome the main challenge for its determination, which
433 is the response of stomatal conductance to water stress. Our derived variable (J_s/D) is a close
434 surrogate of g_s which is widely accepted as one of the most sensitive physiological variables to
435 water stress. Thus, irrigation can be programmed based on a level of g_s indicating moderate
436 water stress.

437

CONCLUSIONS

We found a remarkable good correlation between the dynamics of J_s/D and g_s, both at the diurnal and seasonal levels in trees under three different irrigation regimes, which suggests that J_s/D values could be used to derive g_s in trees under field conditions. Our approach is based on the change in the radial profile pattern of J_s in the trunk which is related and explained by a different response of g_s in sun-exposed and shade leaves to *D,* under contrasting soil water conditions. We have shown that it is possible to estimate g_s in olive trees automatically and in-continuous under field conditions by using sap flux density data directly without need of upscaling to tree transpiration. Considering that automatic and continuous records of J_s/D can be easily obtained and g_s is one of the best plant-based water stress indicators, our findings have a great potential to improve irrigation scheduling in fruit tree orchards. Apart from irrigation scheduling purposes, our approach could also be used in plant physiology studies on plant response to water stress, since the automatic and continuous monitoring of g_s from sap flow related measurements will allow the maintenance of targeted levels of stress as a function of g_s. The value of g_s is a good reference parameter for moderate, mild and severe levels of water stress and the pool of physiological mechanisms of response to water stress associated with them. Still, further studies are required both to understand the hydraulic links between radial variation of sap flux density and the behavior of stomata in the canopy, and to assess whether the method is applicable to species with different characteristics than olive, with larger leaves, closer canopies or different hydraulic functioning.

Acknowledgments

This experiment was funded by the Spanish Ministry of Science and Innovation, research project AGL2009-11310/AGR and by the Junta de Andalucía (research project AGR-6456). Dr.

463 Hernandez-Santana benefited from a Juan de la Cierva postdoctoral research fellowship from
464 the Spanish Ministry of Science and Innovation. Thanks are due to the owners of Internacional
465 Olivarera, S.A.U. (Interoliva), for allowing us to make the experiments in the Sanabria orchard.

466

467 **References**

468 Allen, J., Grime, L., 1995. Measurements of transpiration from Savannah shrubs using sap flow
469 gauges. Agric. For. Meteorol. 1923, 23–41.

470 Alvarado-Barrientos, M.S., Hernandez-Santana, V., Asbjornsen, H., 2013. Variability of the
471 radial profile of sap velocity in *Pinus patula* from contrasting stands within the seasonal cloud
472 forest zone of Veracruz, Mexico. Agric. For. Meteorol. 168, 108–119.

473 Beauchamp, K., Mencuccini, M., Perks, M., Gardiner, B., 2013. The regulation of sapwood area,
474 water transport and heartwood formation in Sitka spruce. Plant Ecol. Divers. 6, 45–56.

475 Brodribb, T.J., 2009. Xylem hydraulic physiology: The functional backbone of terrestrial plant
476 productivity. Plant Sci. 177, 245–251.

477 Buckley, T.N., Mott, K. a, 2013. Modelling stomatal conductance in response to environmental
478 factors. Plant. Cell Environ. 36, 1691–9.

479 Čermák, J., Nadezhdina, N., Meiresonne, L., Ceulemans, R., 2008. Scots pine root distribution
480 derived from radial sap flow patterns in stems of large leaning trees. Plant Soil 305, 61–75.

481 Chalmers, D.J., Mitchell, P.D., van Heek, L., 1981. Control of peach tree growth and
482 productivity by regulated water supply, tree density and summer pruning. J. Am. Soc. Hortic.
483 Sci. 106, 307–312

484 Díaz-Espejo, A, Walcroft, a S., Fernández, J.E., Hafridi, B., Palomo, M.J., Girón, I.F., 2006.
485 Modeling photosynthesis in olive leaves under drought conditions. Tree Physiol. 26, 1445–56.

486 Diaz-Espejo, A., Buckley, T.N., Sperry, J.S., Cuevas, M.V., de Cires, A., Elsayed-Farag, S., Martin-
487 Palomo, M.J., Muriel, J.L., Perez-Martin, A., Rodriguez-Dominguez, C.M., Rubio-Casal, A.E.,
488 Torres-Ruiz, J.M., Fernández, J.E., 2012. Steps toward an improvement in process-based
489 models of water use by fruit trees: A case study in olive. Agric. Water Manag. 114, 37–49.

490 Dye, P.J., B.W. Olbrich and A.G. Poulter. 1991. The influence of growth rings in *Pinus patula* on
491 heat pulse velocity and sap flow measurement. J. Exp. Bot. 42:867–870

492 Egea, G., Verhoef, A., Vidale, P.L., 2011. Towards an improved and more flexible
493 representation of water stress in coupled photosynthesis-stomatal conductance models. Agric.
494 For. Meteorol. 151, 1370–1384.

495 Fernández, J.E., Moreno, F., Giron, I.F., Blazquez, O.M., 1997. Stomatal control of water use in
496 olive tree leaves. Plant Soil 190, 179–192.

497 Fernández J.E., Palomo M.J., Diaz-Espejo A., Girón I.F. 2003. Influence of partial soil wetting on
498 water relation parameters of the olive tree. Agronomie 23, 545-552.

499 Fernández, J.E., Palomo, M.J., Díaz-Espejo, A., Clothier, B., Green, S., Girón, I.F., Moreno, F.,
500 2001. Heat-pulse measurements of sap flow in olives for automating irrigation : tests , root
501 flow and diagnostics of water stress. Agric. Water Manag. 51, 99–123.

502 Fernández, J.E., Durán, P.J., Palomo, M.J., Diaz-Espejo, A., Chamorro, V., Girón, I.F., 2006.
503 Calibration of sap flow estimated by the compensation heat pulse method in olive, plum and
504 orange trees: relationships with xylem anatomy. Tree Physiol. 26, 719–728.

505 Fernández, J.E., Diaz-Espejo, A., D'Andria, R., Sebastiani, L., Tognetti, R., 2008. Potential and
506 limitations of improving olive orchard design and management through modelling. Plant
507 Biosyst. 1, 130-137.

508 Fernández, J.E., Moreno, F., Martín-Palomo, M.J., Cuevas, M.V., Torres-Ruiz, J.M., Moriana, A.,
509 2011. Combining sap flow and trunk diameter measurements to assess water needs in mature
510 olive orchards. Environ. Exp. Bot. 72, 330–338.

511 Fernández, J.E., 2014a. Understanding olive adaptation to abiotic stresses as a tool to increase
512 crop performance. Environ. Exp. Bot. 103, 158–179.

513 Fernández, J.E., 2014b. Plant-based sensing to monitor water stress: Applicability to
514 commercial orchards. Agric. Water Manag. 142, 99–109.

515 Fiora, A., Cescatti, A., 2008. Vertical foliage distribution determines the radial pattern of sap
516 flux density in Picea abies. Tree Physiol. 28, 1317–23.

517 Flexas, J., Scoffoni, C., Gago, J., Sack, L., 2013. Leaf mesophyll conductance and leaf hydraulic
518 conductance: an introduction to their measurement and coordination. J. Exp. Bot. 64, 3965–
519 81.

520 Flexas, J., Medrano, H., 2002. Drought-inhibition of photosynthesis in C3 plants: Stomatal and
521 non-stomatal limitations revisited. Ann. Bot. 89, 183–189.

522 Ford, C.R., Goranson, C.E., Mitchell, R.J., Will, R.E., Teskey, R.O., 2004a. Diurnal and seasonal
523 variability in the radial distribution of sap flow: predicting total stem flow in *Pinus taeda* trees.
524 Tree Physiol. 24, 941–50.

525 Ford, C.R., McGuire, M.A., Mitchell, R.J., Teskey, R.O., 2004b. Assessing variation in the radial
526 profile of sap flux density in *Pinus* species and its effect on daily water use. Tree Physiol. 24,
527 241–249.

528 Gebauer, T., Horna, V., Leuschner, C., 2008. Variability in radial sap flux density patterns and
529 sapwood area among seven co-occurring temperate broad-leaved tree species. Tree Physiol.
530 1821–1830.

531 Granier, a, Anfodillo, T., Sabatti, M., Cochard, H., Dreyer, E., Tomasi, M., Valentini, R., Bréda,
532 N., 1994. Axial and radial water flow in the trunks of oak trees: a quantitative and qualitative
533 analysis. Tree Physiol. 14, 1383–96.

534 Green, S., Clothier, B., Jardine, B., 2003. Theory and Practical Application of Heat Pulse to
535 Measure Sap Flow. Agron. J. 95, 1371–1379.

536 Hetherington, A.M., Woodward, F.I., 2003b. The role of stomata in sensing and driving
537 environmental change. Nature 424, 901–908.

538 Hernandez-Santana, V., David, T.S., Martınez-Fernandez, J., 2008. Environmental and plant-
539 based controls of water use in a Mediterranean oak stand. Forest Ecology Management 255,
540 3707–3715.

541 Hernandez-Santana, V., Hernandez-Hernandez, A., Vadeboncoeur, M., Asbjornsen, H., 2015.
542 Scaling from single-point sap velocity measurements to stand transpiration in a multispecies
543 deciduous forest: uncertainty sources, stand structure effect, and future scenarios. Canadian
544 Journal of Forest Research 45, 1489–1497.

545 Jarvis P.G., 1976. The interpretation of the variations in leaf water potential and stomatal
546 conductance found in canopies in the field. Philosophical Transactions of the Royal Society
547 London, Series B 273, 593–610.

548 Jarvis, P.G., Mcnaughton, K.G., 1986. Stomatal control of transpiration: scaling up from leaf to
549 region. In: Macfadyen, A., Ford, E.D. (Eds.), Advances in Ecological Research. Academic Press,
550 London, pp. 1–49.

551 Jiménez, M.S., Nadezhdina, N., Cermák, J., Morales, D., 2000. Radial variation in sap flow in five
552 laurel forest tree species in Tenerife, Canary Islands. Tree Physiol. 20, 1149–1156.

553 Jones, H.G., 2004. Irrigation scheduling: advantages and pitfalls of plant-based methods. J. Exp.
554 Bot. 55, 2427–2436

555 Leuning R. (1990) Modeling stomatal behavior and photosynthesis of eucalyptus-grandis.
556 Australian Journal of Plant Physiology 17, 159–175.

López-Bernal, Á., Alcántara, E., Testi, L., Villalobos, F.J., 2010. Spatial sap flow and xylem anatomical characteristics in olive trees under different irrigation regimes. Tree Physiol. 30, 1536–1544.

Maton, C., Gartner, B.L., 2005. Do gymnosperm needles pull water through the xylem produced in the same year as the needle? Am. J. Bot. 92, 123–31.

McNaughton, K.G., Jarvis, P.G., 1983. Predicting effect of vegetation changes on transpiration and evaporation. In: Kozlowski, T.T. (Ed.), Water Deficits and Plant Growth, vol. VII. Academic Press, pp. 1–47.

Medrano, H., Escalona, J.M., Bota, J., Gulías, J., Flexas, J., 2002. Regulation of photosynthesis of C3 plants in response to progressive drought: Stomatal conductance as a reference parameter. Ann. Bot. 89, 895–905.

Morales, L. V, Coopman, R.E., Rojas, R., Escandón, A.B., Flexas, J., Galmés, J., García-Plazaola, J.I., Gago, J., Cabrera, H.M., Corcuera, L.J., 2014. Acclimation of leaf cohorts expanded under light and water stresses: an adaptive mechanism of *Eucryphia cordifolia* to face changes in climatic conditions? Tree Physiol. 34, 1305–20.

Moreno, F., Fernández, J.E., Clothier, B., Green, S., 1996. Transpiration and root water uptake by olives. Plant Soil 84, 85–96.

Nadezhdina, N., Cermák, J., Ceulemans, R., 2002. Radial patterns of sap flow in woody stems of dominant and understory species: scaling errors associated with positioning of sensors. Tree Physiol. 22, 907–918.

Nadezhdina, N., Nadezhdin, V., Ferreira, M.I., Pitacco, A., 2007. Variability with xylem depth in sap flow in trunks and branches of mature olive trees. Tree Physiol. 27, 105–13.

Oren, R., Sperry, J.S., Katul, G.G., Pataki, D.E., Ewers, B.E., Phillips, N., Schäfer, K.V.R., 1999. Survey and synthesis of intra- and interspecific variation in stomatal sensitivity to vapour pressure deficit. Plant, Cell Environ. 22, 1515–1526.

Orgaz F, Fereres E (2001) Riego. In: Barranco D, Fernández–Escobar, R, Rallo L (eds) El Cultivo del Olivo, 4th edn. Coedition. Mundi–Prensa and Junta de Andalucía, Madrid, pp 285–306

Peak, D., Mott, K., 2011. A new, vapour-phase mechanism for stomatal responses to humidity and temperature. Plant, Cell Environ. 34, 162–178.

Poyatos, R., Èermák, J.A.N., Llorens, P., 2007. Variation in the radial patterns of sap flux density in pubescent oak (*Quercus pubescens*) and its implications for tree and stand transpiration measurements. Tree Physiol. 537–548.

589 Sancho-Knapik, D., Peguero-Pina, J.J., Flexas, J., Herbette, S., Cochard, H., Niinemets, U., Gil-
590 Pelegrin, E., 2014. Coping with low light under high atmospheric dryness: shade acclimation in
591 a Mediterranean conifer (*Abies pinsapo* Boiss.). Tree Physiol. 34, 1321–

592 Shinohara, Y., Tsuruta, K., Ogura, A., Noto, F., Komatsu, H., Otsuki, K., Maruyama, T., 2013.
593 Azimuthal and radial variations in sap flux density and effects on stand-scale transpiration
594 estimates in a Japanese cedar forest. Tree Physiol. 1–9.

595 Swanson, R.H., 1994. Significant historical developments in thermal methods for measuring
596 sap flow in trees. Agric. For. Meteorol. 72, 113–132.

597 Tognetti, R., Giovannelli, A., Lavini, A., Morelli, G., Fragnito, F., d'Andria, R.,2009. Assessing
598 environmental controls over conductances through the soil–plant–atmosphere continuum in
599 an experimental olive tree plantation of southern Italy. Agric. For. Meteorol. 149, 1229–1243.

600 Vandegehuchte, M.W., Braham, M., Lemeur, R., Steppe, K., 2012. The importance of sap flow
601 measurements to estimate actual water use of meski olive trees under different irrigation
602 regimes in Tunisia. Irrig. Drain. 61, 645–656.

603 Wullschleger, S.D., Meinzer, F.C., Vertessy, R.A., 1998. A review of whole-plant water use
604 studies in trees. Tree Physiol.

605 Zhang, H., Simmonds, L.P., Morison, J.I.L., 1997. Estimation of transpiration by single trees :
606 comparison of sap flow measurements with a combination equation. Agric. For. Meteorol. 87,
607 155–169.

608

609 **Tables**

610 Table 1. Summary of measurements and sample sizes conducted in the two studied orchards.

	La Hampa		**Sanabria**	
	# Trees	# Leaves	# Trees	# Leaves
Sap flow probes	2		9	
Regular stomatal conductance	2		18	18 (1 leaves/tree)
Daily cycles of g_s on SUN-SHADE leaves	2	4	2	8 (4 leaves/tree)

611

612

613

Figure legends

Figure 1. a) Diurnal course of air vapor pressure deficit (D). Grey squares represent *D* at the three times of the day plotted in b) panel. b) Example of the diurnal change in the radial pattern of sap flux density (J_s) from probes in a well-watered olive tree (treatment WW; see text for details) at Sanabria orchard on 25 June 2012 (DOY 177) at three different times of the day. It can be observed how J_s at 20 mm increased relatively more than J_s at 10 mm as *D* increased during the day.

Figure 2. Relationship between stomatal conductance (g_s) and sap flux density (J_s) at 5 mm below the cambium for SUN leaves (J_{s1}) and 10 mm below cambium for SHADE leaves (J_{s2}) divided by the air vapor pressure deficit (*D*). Data in panels a) and b) belong to Sanabria orchard and show two different days, on DOY 177 both trees were well irrigated but in DOY 216 one tree was well-watered (WW) and the other one was water-stressed (WS). In c) and d) we have the results of La Hampa orchard representing one single day. In both cases black symbols represent sun leaves and white symbols shaded leaves. Trees under well-watered conditions (WW) are represented in upper panels a) and c), and trees under water stress (WS) in lower panels b) and d). Each point represents the average of four g_s measurements. All fitted curves were statistically significant (P<0.0001).

Figure 3. Response of stomatal conductance (g_s) to the natural logarithm of air vapor pressure deficit (Ln*D*) in sun exposed, young leaves (SUN, black circles) and shaded, old leaves (SHADE, white circles). Data in panels a) and b) belong to Sanabria orchard and show two different days, and c) and d) to La Hampa orchard representing one single day. Trees under well-watered conditions (WW) are represented in upper panels a) and c) and trees under water stress (WS) in lower panels b) and d). Each point represents the average of four g_s measurements taken at different times of the day from 7:00 to 18:30 GMT on the 3rd of August of 2012 (DOY 216). The curves were significant (P<0.05) as fitted using the g_s values of central day hours from 8.30 to 15.30 GMT to avoid hysteresis. Grey arrows indicate the course of g_s along the day facilitating the visualization of hysteresis.

Figure 4. Relationship between the natural logarithm of air vapor pressure deficit (Ln*D*) and the ratio of sap flux density (J_s) measured at 5 mm (J_{S1}) and 10 mm (J_{S2}) below the cambium. Data in panels a) and b) belong to Sanabria orchard and show two different days, and c) and d) to La Hampa orchard representing one single day. Trees under well-watered conditions (WW) are represented in upper panels a) and c) and trees under water stress (WS) in lower panels b) and d). In panel a) and b) white circles represent DOY 177 and black circles DOY 216. All fitted curves were statistically significant (*P*<0.01).

Figure 5. Temporal course of a) air vapor pressure deficit (*D*), b) solar radiation (R_s) and c) relative extractable water (REW) in the three irrigation treatments at Sanabria experimental orchard. In panel c) black circles are REW in full irrigation treatment (FI), white circles are REW in the deficit irrigation treatment in which only 60% of irrigation needs were covered (60RDI) and black triangles are REW in the irrigation treatment where only 30% of the irrigation needs were replaced (30RDI) along the long-term experiment.

Figure 6. Lines show the temporal changes of stomatal conductance (g_s) calculated from sap flow measurements applying the relationship found in Fig. 2 between g_s and sap flux density (J_s) measured at 5 mm below the cambium (J_{S1}) divided by air vapor pressure deficit (*D*). Panels represent: (a) full irrigation treatment (FI), (b) deficit irrigation treatment in which only 60% of irrigation needs were replaced by irrigation (60RDI) and (c) deficit irrigation treatment in which only 30% of irrigation needs were replaced by irrigation (30RDI) trees (grey line). Black circles are the average of two independent g_s measurements at 8:30 GMT as explained in Material and Methods. Stomatal conductance estimated from J_s/D at 8:30 GMT, the same time that g_s was measured, is represented for comparison purposes.

Figure 7. Comparison of measured stomatal conductance (g_s) and calculated g_s through sap flux density/air vapour pressure deficit (J_s/D) relationship for all days represented in Fig. 6 and all three treatments as indicated in the legend. P<0.0001; r^2= 0.86.

661 ADDITIONAL FIGURES (not for publication)

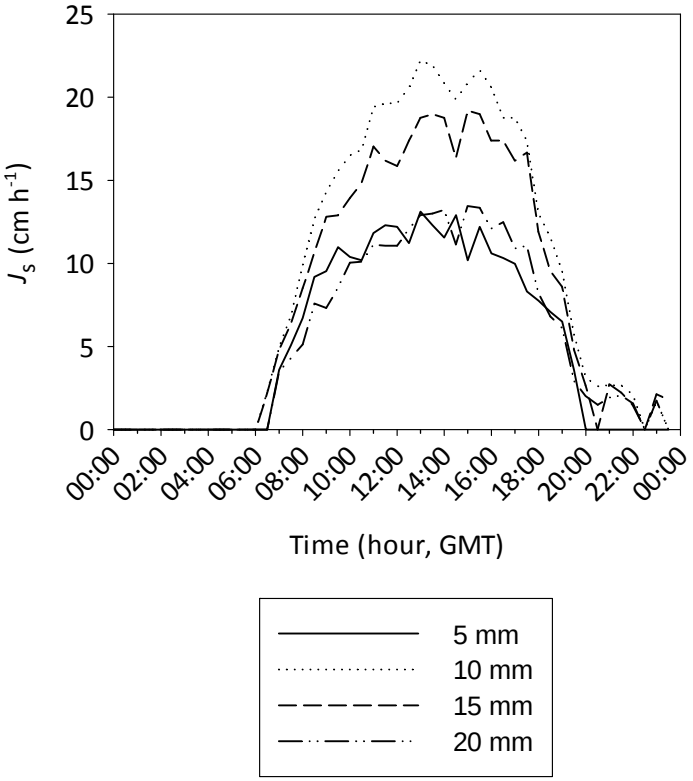

662

663 Extra figure 1. Diurnal evolution of sap flux density (J_s) at four different depths below the
664 cambium in the sampled tree shown in Fig. 1.

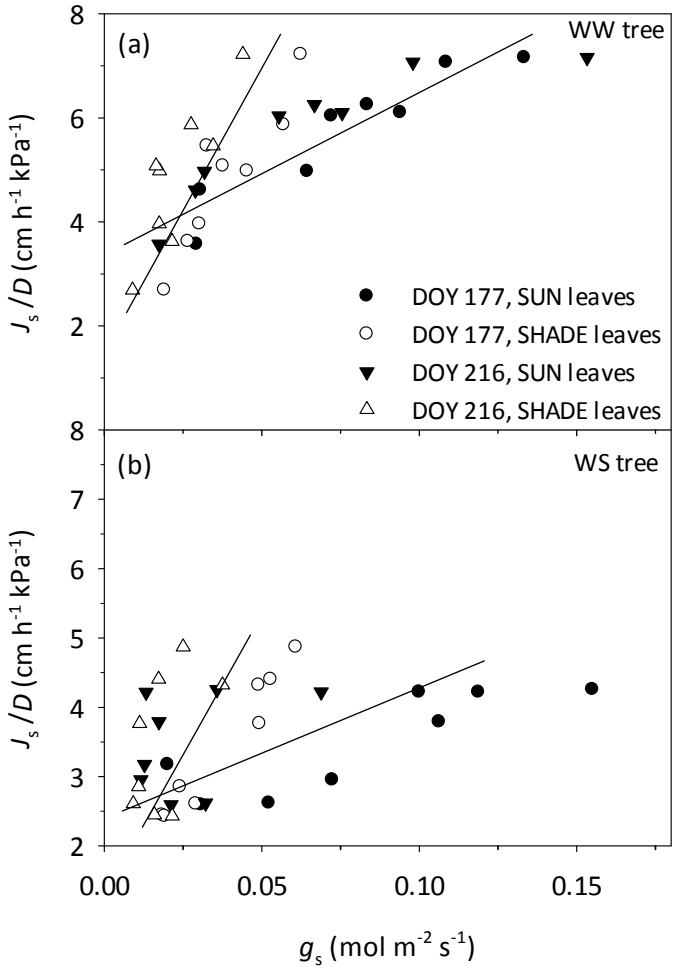

665

666 Extra Figure 2. Stomatal conductance values of SUN leaves correlated to J_s values at 10 mm
667 (J_{s2}) and g_s values of SHADE leaves correlated to J_s values at 5 mm (J_{s1}). In the table below are
668 shown the coefficients of determination to demonstrate that g_s SUN correlated better with J_{s1},
669 and g_s SHADE with J_{s2}. As commented in our reply to reviewers, we consider that this plot and
670 table do not deserve publication.

	g_s SUN		g_s SHADE	
	J_{s1}	J_{s2}	J_{s1}	J_{s2}
WW tree	0.80	0.71	0.75	0.84
WS tree	0.84	0.72	0.77	0.82

671

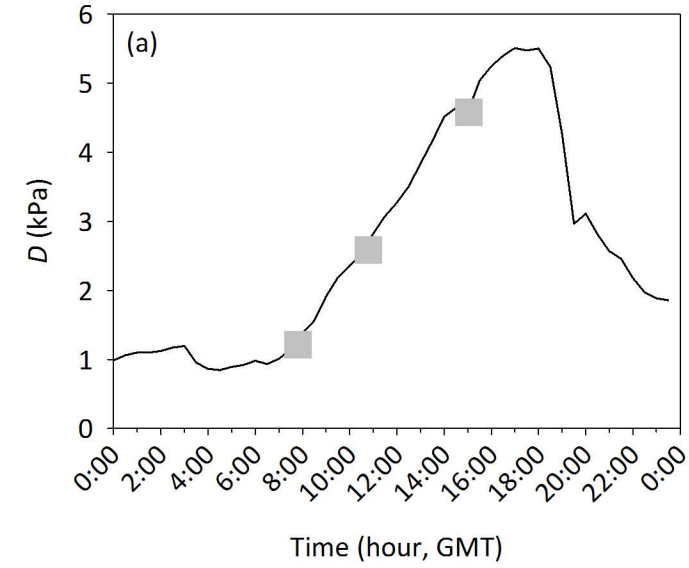
(a)
D (kPa)
0
1
2
3
4
5
6
0:00
2:00
4:00
6:00
8:00
10:00
12:00
14:00
16:00
18:00
20:00
22:00
0:00
Time (hour, GMT)

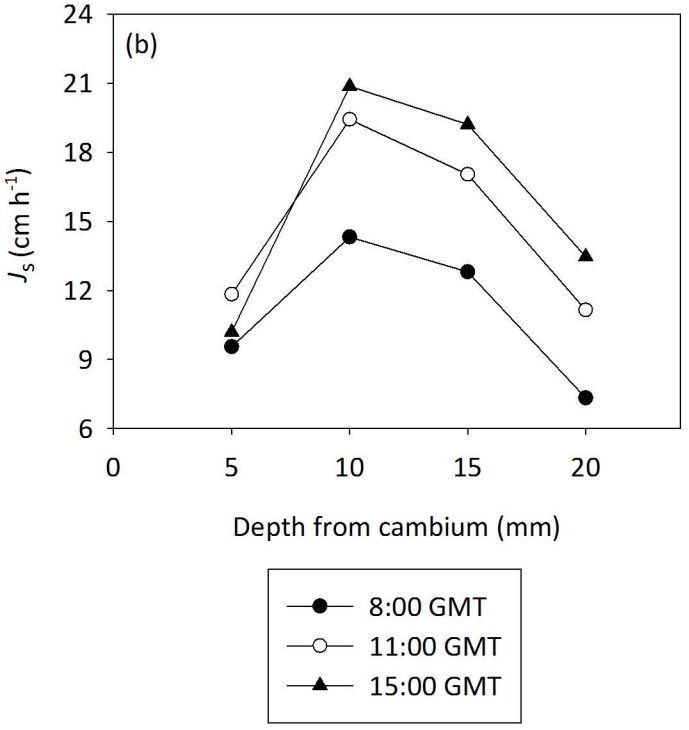
(b)
J_S (cm h^{-1})
6
9
12
15
18
21
24
0
5
10
15
20
Depth from cambium (mm)
8:00 GMT
11:00 GMT
15:00 GMT

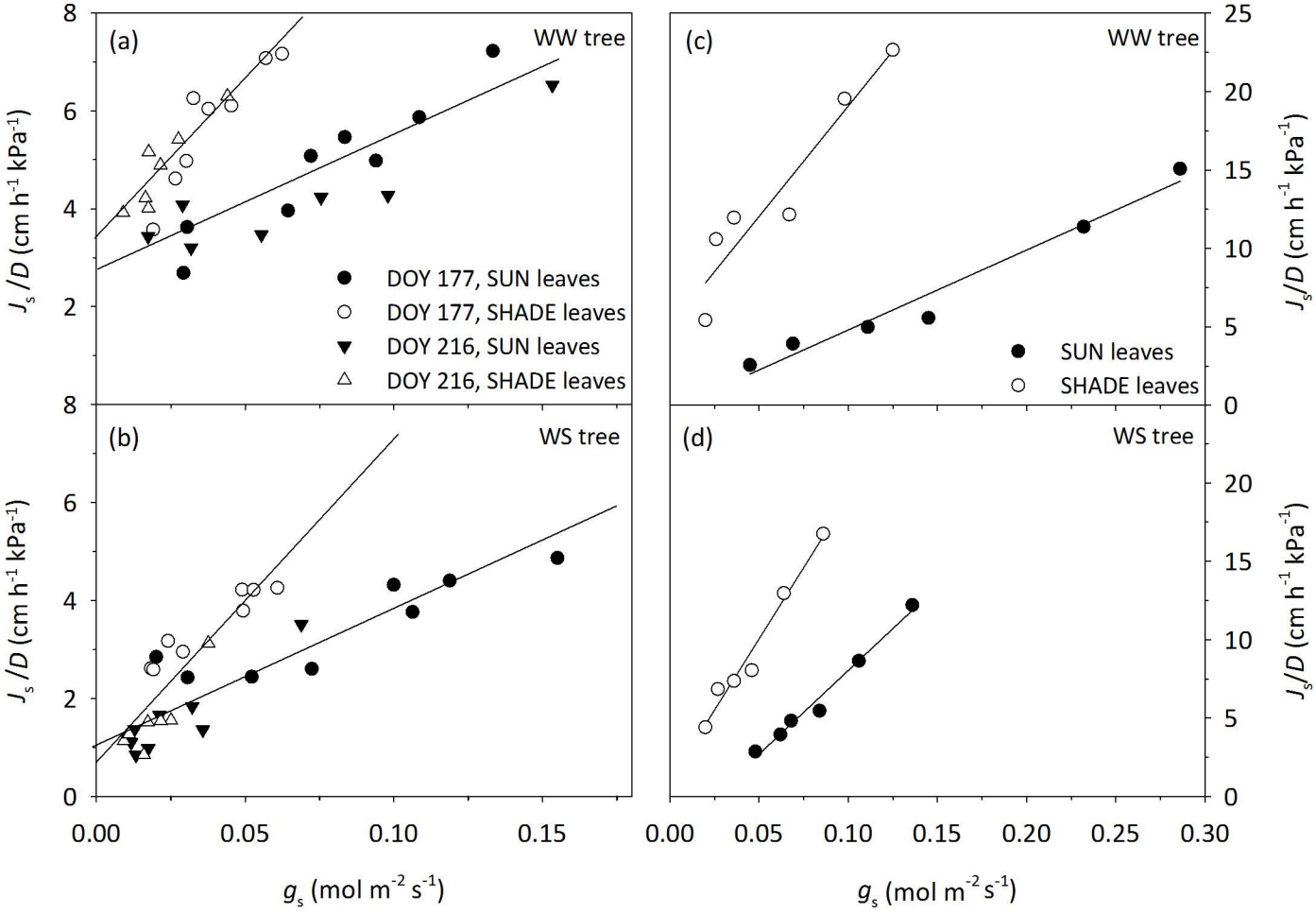
(a)
WW tree
(b)
WS tree
(c)
WW tree
(d)
WS tree
DOY 177, SUN leaves
DOY 177, SHADE leaves
DOY 216, SUN leaves
DOY 216, SHADE leaves
SUN leaves
SHADE leaves
J_s/D (cm h^{-1} kPa^{-1})
g_s (mol m^{-2} s^{-1})
0.00
0.05
0.10
0.15
0.20
0.25
0.30
0
2
4
6
8
0
5
10
15
20
25

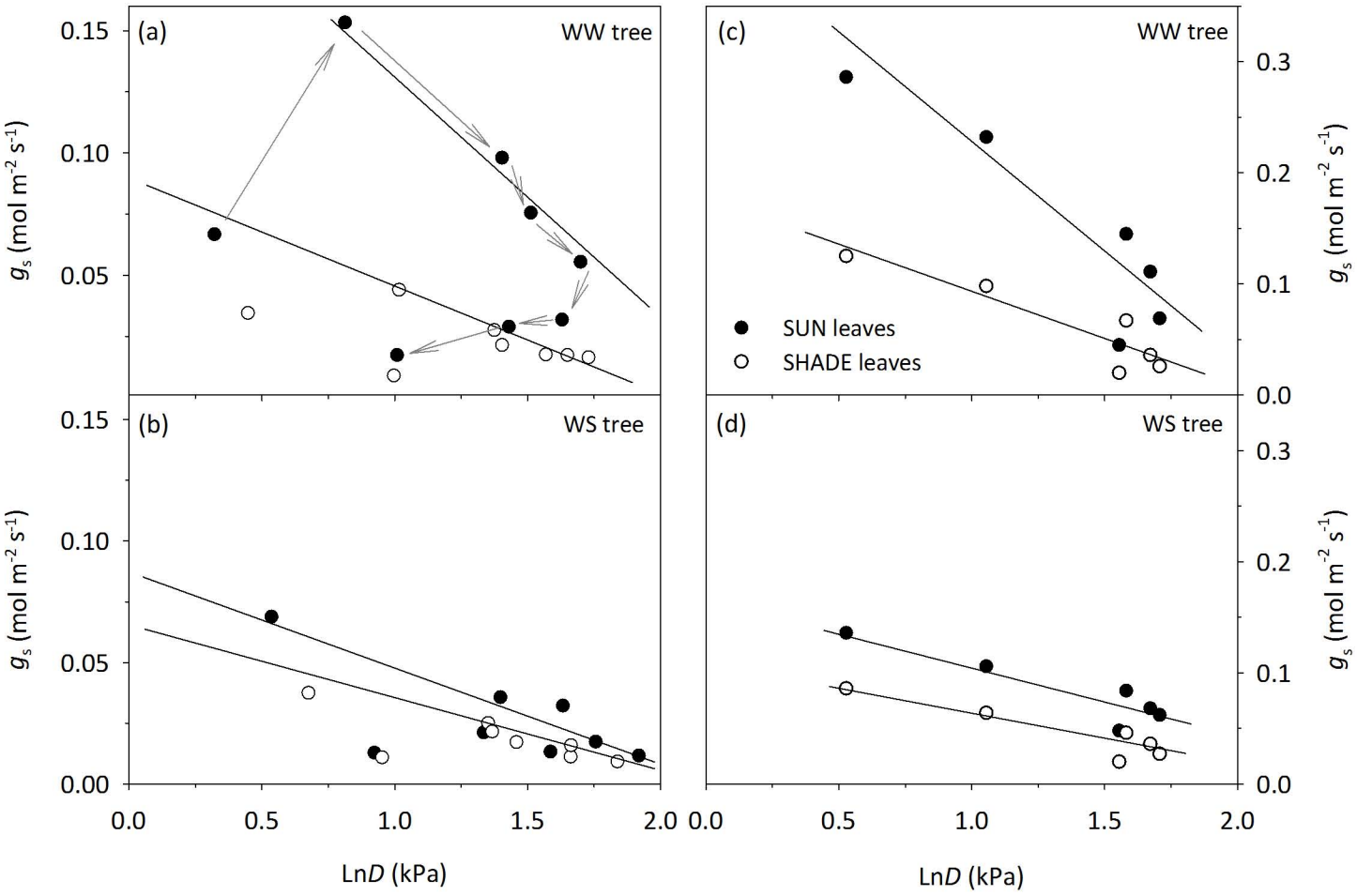
(a)
WW tree
(b)
WS tree
(c)
WW tree
(d)
WS tree
SUN leaves
SHADE leaves
g_s (mol m^{-2} s^{-1})
LnD (kPa)
0.15
0.10
0.05
0.00
0.3
0.2
0.1
0.0
0.5
1.0
1.5
2.0

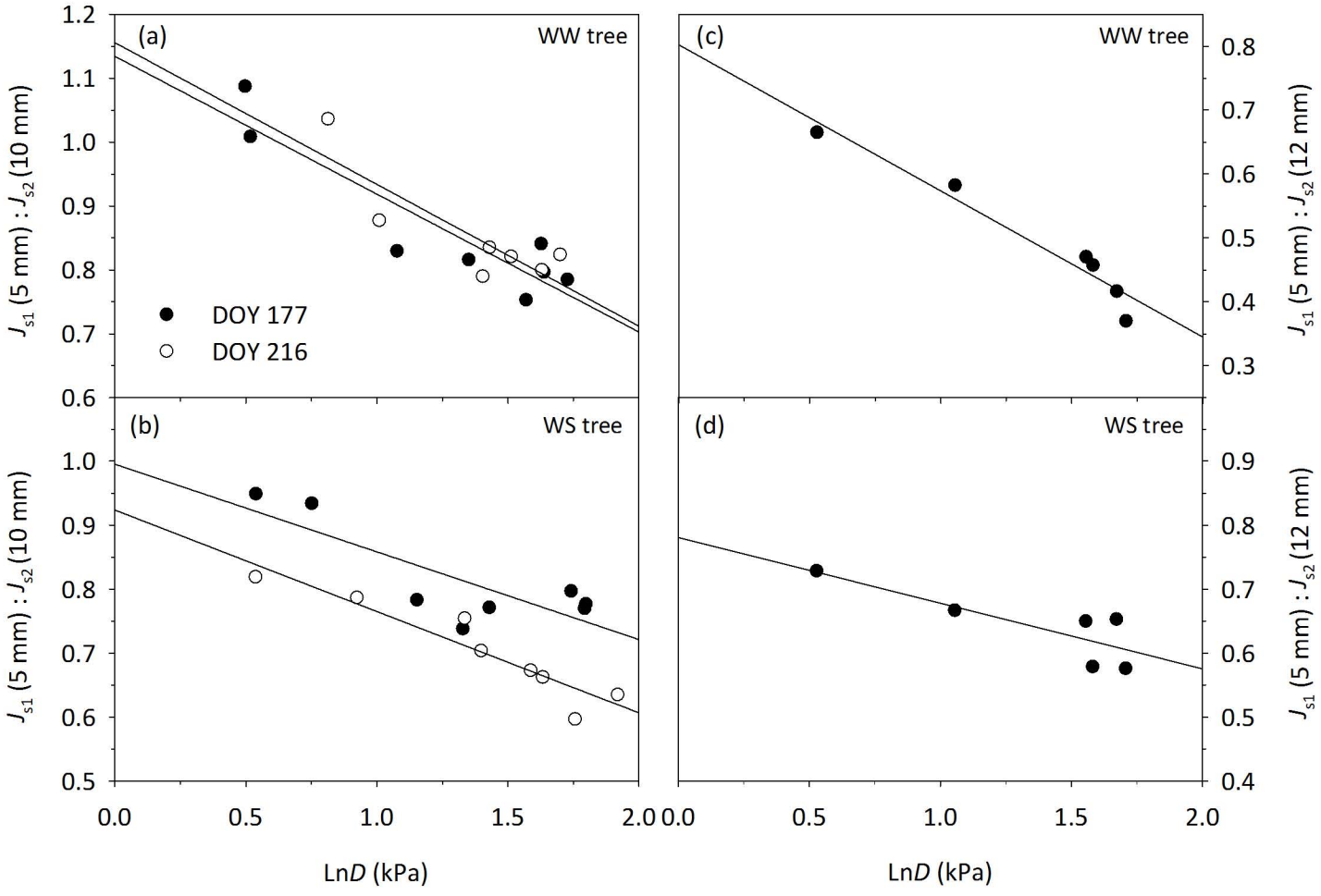
(a)
WW tree
DOY 177
DOY 216
(b)
WS tree
(c)
WW tree
(d)
WS tree
J_{s1} (5 mm) : J_{s2} (10 mm)
J_{s1} (5 mm) : J_{s2} (12 mm)
LnD (kPa)
LnD (kPa)

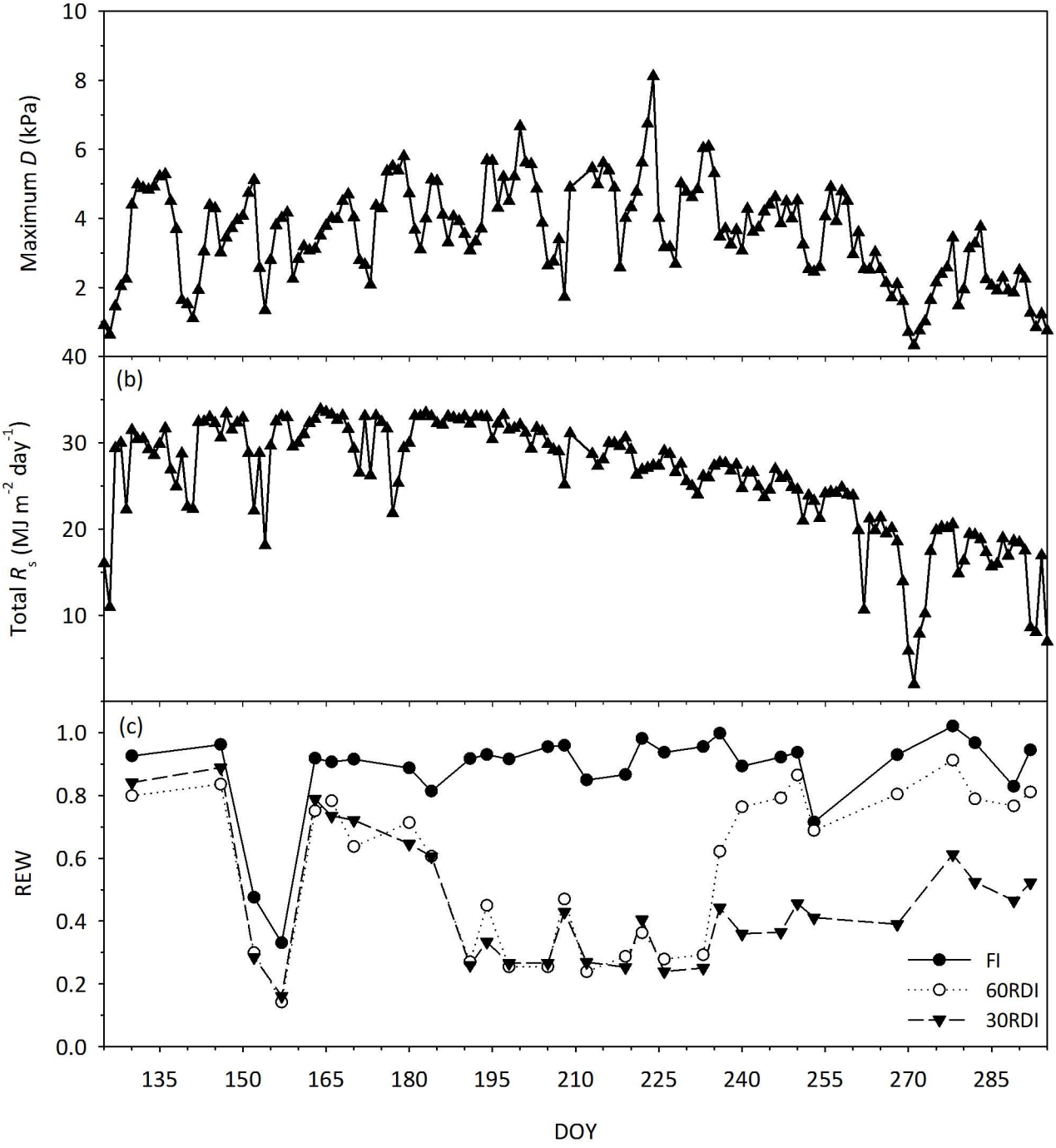
Maximum D (kPa)
Total R_s (MJ m^{-2} day^{-1})
REW
(b)
(c)
FI
60RDI
30RDI
DOY

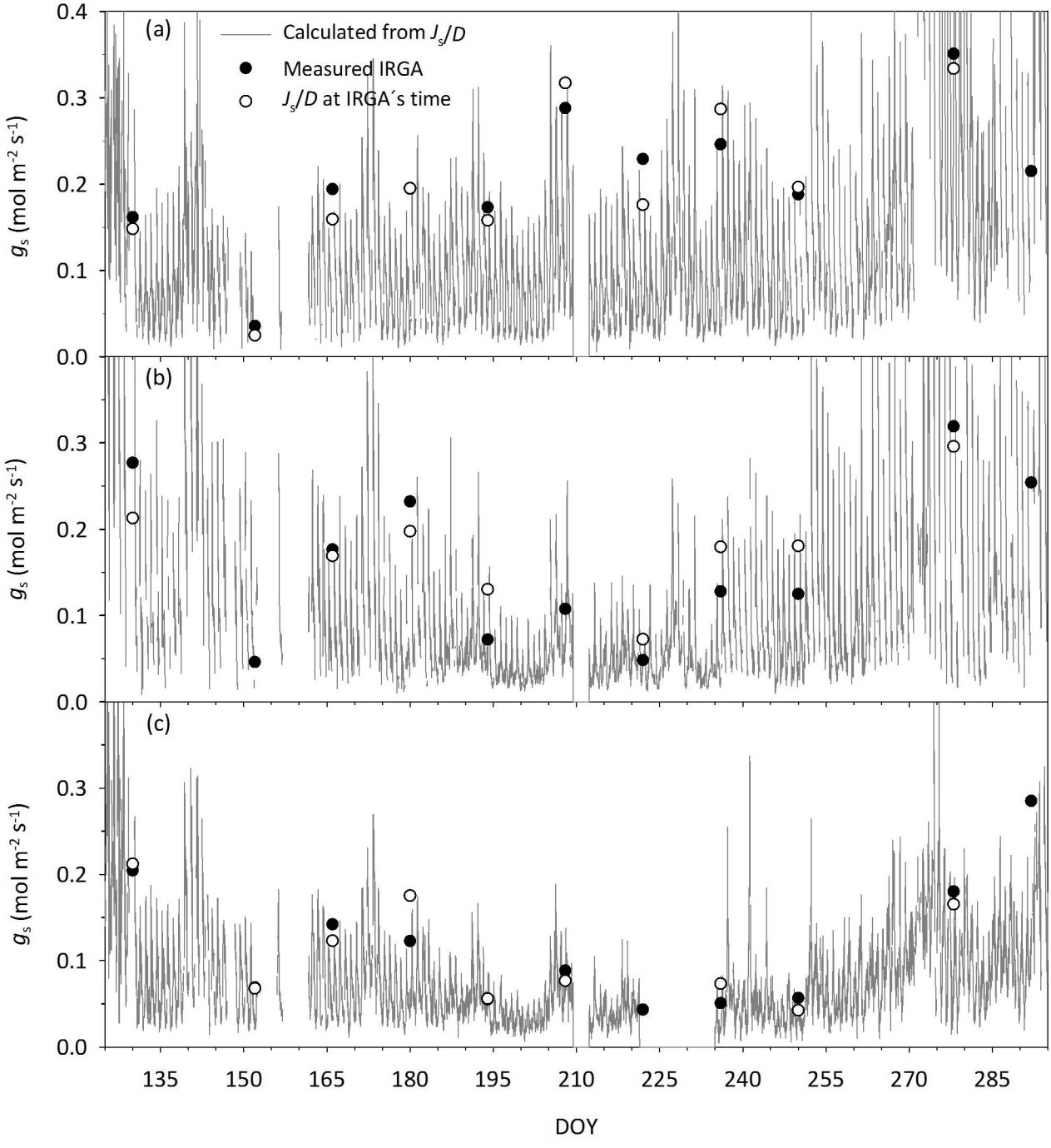
(a)
Calculated from J_s/D
Measured IRGA
J_s/D at IRGA´s time
(b)
(c)
g_s (mol m^{-2} s^{-1})
0.0
0.1
0.2
0.3
0.4
135
150
165
180
195
210
225
240
255
270
285
DOY

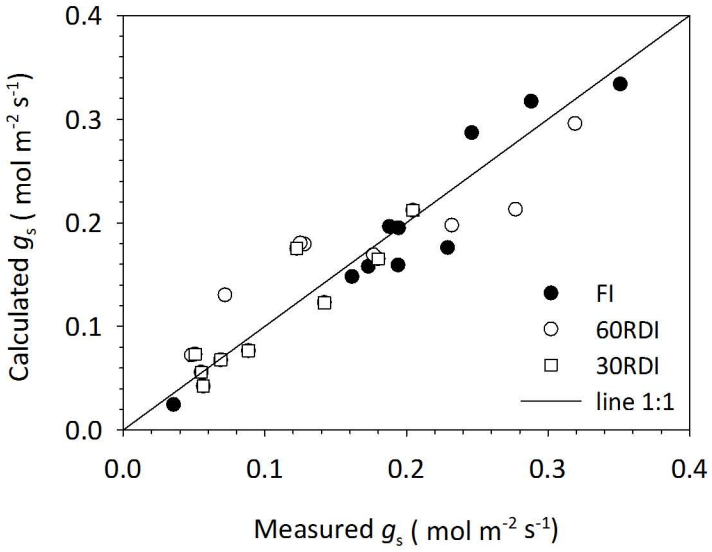
0.4
0.3
0.2
0.1
0.0
0.0
0.1
0.2
0.3
0.4
Calculated g_s (mol m^{-2} s^{-1})
Measured g_s (mol m^{-2} s^{-1})
FI
60RDI
30RDI
line 1:1